





REVIEW ARTICLE

Mechanical characterization and design of biomaterials for nucleus pulposus replacement and regeneration

Zhuoqi Lucas Li¹  | Qiuji Lu¹ | John Robert Honiball¹ |
Sandra Hiu-Tung Wan¹  | Kelvin Wai-Kwok Yeung^{1,2}  |
Kenneth Man-Chee Cheung^{1,3} 

¹Department of Orthopaedics & Traumatology, The University of Hong Kong, Hong Kong, China

²Shenzhen Key Laboratory for Innovative Technology in Orthopaedic Trauma, The University of Hong Kong Shenzhen Hospital, Shenzhen, China

³Department of Orthopaedics and Traumatology, The University of Hong Kong-Shenzhen Hospital, Shenzhen, China

Correspondence

Kenneth Man-Chee Cheung, Department of Orthopaedics & Traumatology, The University of Hong Kong, Hong Kong, China.

Email: cheungmc@hku.hk

Funding information

HKU-SZH Fund for Shenzhen Key Medical Discipline (SZXK2020084); Sanming Project of Medicine in Shenzhen "Team of Excellence in Spinal Deformities and Spinal Degeneration" (SZSM201612055); The University of Hong Kong Seed Fund for Translational and Applied Research (104006073)

Abstract

Biomaterials for nucleus pulposus (NP) replacement and regeneration have great potential to restore normal biomechanics in degenerated intervertebral discs following nucleotomy. Mechanical characterizations are essential for assessing the efficacy of biomaterial implants for clinical applications. While traditional compression tests are crucial to quantify various modulus values, relaxation behaviors and fatigue resistance, rheological measurements should also be conducted to investigate the viscoelastic properties, injectability, and overall stability upon deformation. To recapitulate the physiological *in vivo* environment, the use of spinal models is necessary to evaluate the risk of implant extrusion and the restoration of biomechanics under different loading conditions. When designing devices for NP replacement, injectable materials are ideal to fully fill the nucleus cavity and prevent implant migration. In addition to achieving biocompatibility and desirable mechanical characteristics, biomaterial implants should be optimized to avoid implant extrusion or re-herniation post-operatively. This review discusses the most commonly used testing protocols for assessing mechanical properties of biomaterial implants and serves as reference material for enabling researchers to characterize NP implants through a unified approach whereby newly developed biomaterials may be compared and contrasted to existing devices.

KEYWORDS

biomaterials, mechanical characterization, mechanical properties, methodologies, nucleus pulposus

1 | INTRODUCTION

Intervertebral disc (IVD) degeneration is commonly observed across populations and is closely related to factors such as aging, abnormal mechanical loading and genetics.¹ One consequence of IVD degeneration is lower back pain, which is considered to be one of the most debilitating conditions causing severe stress on both the patient and public health

services.² With the global rise in the human population and aging societies with increasing life expectancies, it is reasonable to predict IVD degeneration-related diseases will affect increasingly more individuals and social healthcare systems in the near future.

In the IVD, a gelatinous proteoglycan-rich nucleus pulposus (NP) is confined peripherally by a collagen-rich annulus fibrosus (AF) and is sandwiched by cartilaginous vertebral endplates on the superior and

This is an open access article under the terms of the [Creative Commons Attribution](https://creativecommons.org/licenses/by/4.0/) License, which permits use, distribution and reproduction in any medium, provided the original work is properly cited.

© 2023 The Authors. *Journal of Biomedical Materials Research Part A* published by Wiley Periodicals LLC.

inferior surfaces.³ The unique mechanical properties of the NP and AF are fundamental in sustaining the high pressure experienced by IVDs during daily activities. Progression of degeneration is associated with a reduction in proteoglycan synthesis, coupled with a decrease in collagen type II.⁴ In place of collagen type II, increased levels of collagen types I and III, as well as matrix metalloproteinase 12 (MMP12), a matrix degradation enzyme, are produced. These changes lead to the loss of mechanical properties of the IVD, and structural wear gradually appears.⁵ At the same time, glycosaminoglycan content also decreases, leading to dehydration and a reduction in the intrinsic swelling capacity of the NP.⁶ Due to the decrease in osmotic pressure and the indistinguishable NP-AF border, the load transfer function of the NP is impaired, with higher stress experienced by the outer AF region of the IVD; causing subsequent disc height reduction.^{7,8} Figure 1 shows that as the degenerative process progresses, leakage of the central NP from the cracks of the AF (herniated disc) enables immune cell activation and infiltration, resulting in the release of cytokines and neurogenic factors which cause severe lower back pain.⁹ In the case of severe degeneration, compression on the nerve roots in the region of the bulged or herniated discs may also contribute to lower back pain.^{6,10}

Several surgical procedures exist for the treatment of degenerated IVDs. Spinal fusion involves fusing the two vertebrae on either side of the disc together. Although this technique can alleviate short-term pain relief, the procedure limits the spinal motion, and normal biomechanics of the motion segment cannot be restored.¹¹ Accelerated degeneration of the segment adjacent to the lumbar fusion has also been reported.¹² In discectomy (partial removal of a degenerated disk), IVD instability often occurs, leading to long-term complications.¹³ Nucleotomy (removal of the NP component of the IVD) has been demonstrated to be effective in the reduction of herniation-induced pain.¹⁴ However, following denucleation of the IVD, the inner margin of the AF bulges inwards due to the lack of support from the NP; this abnormal bulging behavior leads to further degeneration of the IVD and loss of spinal stability postoperatively.^{14,15}

One solution proposed to treat degenerated IVDs and at the same time restore the normal biomechanics of the spine is by implementing

NP replacement materials. With suitable stiffness ranges, NP replacement materials are capable of preventing the inward bulging of the AF after denucleation of the IVD, which prevents further AF degeneration.¹⁵ Several studies have demonstrated the effectiveness of NP implants in restoring normal spinal range of motion, size of neutral zone, and disc height.^{14,16,17} Despite being a worldwide research topic of interest spanning over two decades, clinical use of NP implants has not been widely implemented. A core challenge in designing a desirable NP implant lies in the precise mechanical property requirements. For example, an overly stiff material leads to stress shielding, resulting in an increased risk for endplate subsidence.^{16,17} Contrastingly, a soft (less stiff) material increases the load experienced by the AF, promoting IVD degeneration. It is also easier for a soft material to be extruded out of the disc from the annulus incision or fragment inside the patient body.^{18,19}

To date, biomaterials for the treatment of degenerated NP are either synthetically manufactured permanent acellular implants²⁰ or degradable materials which rely on cell growth and proliferation to form neo-NP tissue at the site of degeneration to illicit repair.²¹ In all NP replacement strategies, the mechanical properties of biomaterials are of great significance. Simple uniaxial compression tests are far from adequate when considering the six degrees of freedom motions (flexion, extension, right and left lateral bending, compression, and axial rotation) experienced in the human spine.²² Often times, the complications and failures of NP implants are largely attributed to the complex physiological loading environments experienced in day-to-day activities.²³ Figure 2 highlights the major developmental stages for creating a functional NP implant. In this article, with papers systematically collected from three major databases, essential parameters and methodologies to characterize the mechanical properties of NP replacement/regenerative biomaterials are reviewed. General concepts, testing methods, commonly overlooked details and biomaterial designs are all included as part of the discussion. For completeness, techniques to demonstrate biomaterial biocompatibility and efficacy are also touched upon. With the data and testing methods collected from a wide selection of studies, researchers can easily compare their newly designed biomaterials with those which have been previously developed and which demonstrate several limitations observed in clinical

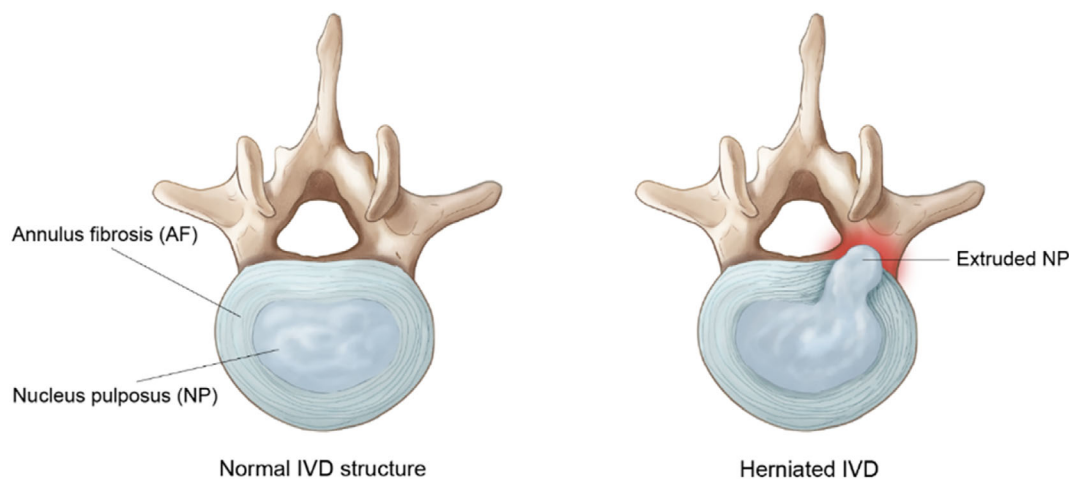


FIGURE 1 Schematic illustration of a normal/healthy IVD and a herniated IVD after degeneration.

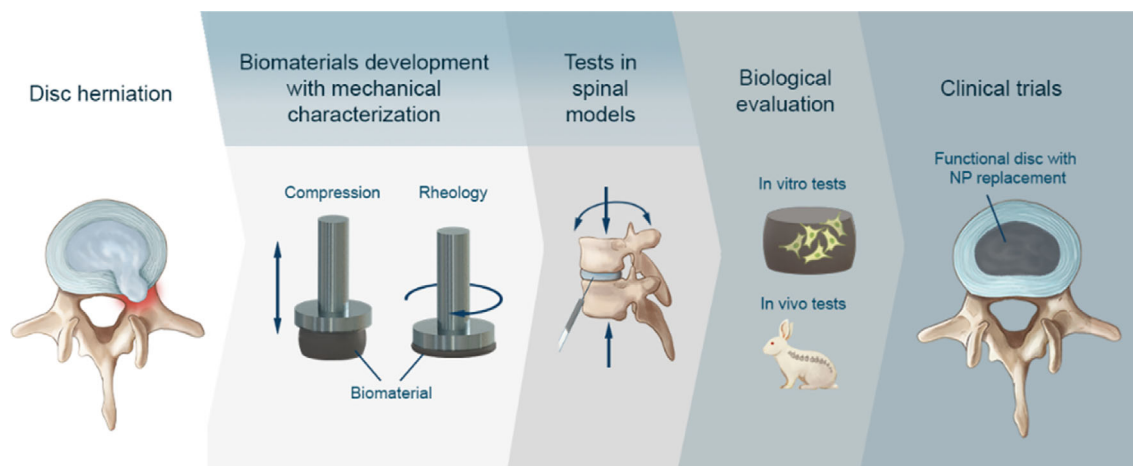


FIGURE 2 Major stages in the development of an NP implant.

scenarios. The ultimate goal of this comprehensive review is to serve as a library of information (toolkit) for researchers who aim to develop functional NP implants which may eventually achieve clinical success.

2 | INTRINSIC FUNCTIONS AND PROPERTIES OF THE NUCLEUS PULPOSUS: WHAT TO MIMIC?

Compared with the AF, the NP plays a relatively minor role in providing internal pressure and load transfer functionality of the IVD.²⁴ The main purpose of the NP in the central region of the IVD is to provide mobility and to dissipate energy under large physiological deformation at high loading frequencies, whereas at low frequencies, the intrinsic fluid flow is enhanced.^{25,26} In addition to aiding the central disc to maintain its height, the presence of the NP affects the deformation and bulging behavior of the inner AF.¹⁴ Numerous studies have shown that the removal of the NP leads to the inward bulging of the AF, resulting in increased stress experienced by the AF which may lead to further fibrous ring rupture and herniation.^{27,28}

During daily activities and depending on the posture of the individual, IVDs experience various loading conditions with different levels of pressure. Wilke et al. measured the *in vivo* intradiscal pressure and found that from lying supine to lifting a 20 kg object, the pressure experienced by the IVD ranged from 0.1 MPa to over 2 MPa.²⁹ Table 1 highlights the changes in IVD pressure during daily activities. Apart from the high intradiscal pressure, the biomechanics in a functional spinal unit are complex, and several aspects should be considered when designing experiments to characterize NP implants. Firstly, loading conditions vary according to different activities. Compression is the most common loading condition experienced by IVDs, and shear is also frequently observed within spinal segments during bending and torsion.³⁰ With compression and shear being the major loading conditions experienced by IVDs several mechanical properties in biomaterials need to be characterized in order to mimic the physiological function of native NPs. Primarily, the material developed should be able to withstand high pressures without risk of failure inside the cavity, or extrusion out of the AF incision. This requires the

TABLE 1 Pressure experienced by IVD during daily activities.²⁹

Situations	Pressure (MPa)
Sleeping (from lying to turning around)	0.10–0.80
Sitting (from slouched into the chair to flexion)	0.27–0.83
Standing (from relaxed to bent forward)	0.50–1.10
Walking (from flat ground to climbing stairs)	0.53–0.70
Jogging with different shoes	0.35–0.95
Lifting a 20 kg object with various positions of posture	1.70–2.30

material to have sufficient mechanical strength to resist pressure. In addition, the stiffness/modulus of the implant should be within a certain range in order to restore the normal biomechanics of the spine and prevent the inward bulging of the AF. The native NP is a viscoelastic tissue which demonstrates both fluid and solid-like characteristics.³¹ Henceforth, the viscoelastic properties of potential biomaterials should also be assessed through various compressive (creep and relaxation) and/or rheological tests. An ideal permanent implant should maintain its mechanical properties in the long term. Conversely, a biodegradable material requires the rate of degradation to be in-line with that of native tissue formation and maturation. In the subsequent sections, characterization techniques conducted to evaluate material mechanical properties and various NP designs tailored to facilitating replacement/regeneration will be reviewed and discussed.

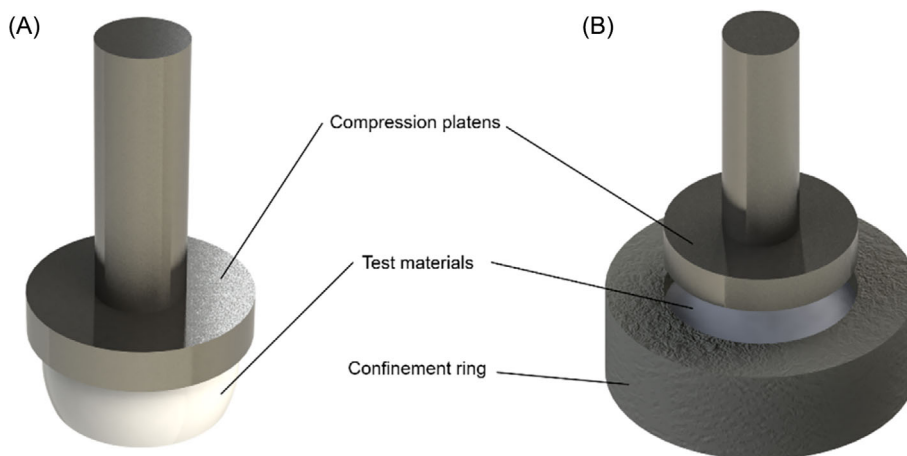
3 | MECHANICAL TESTS FOR CHARACTERIZATION – HOW TO EVALUATE?

3.1 | Compression

3.1.1 | Unconfined compression tests – compressive strength

As its name suggests, the unconfined compression test involves the compression of the test material without any confinement (Figure 3A).

FIGURE 3 Two modes employed in compression testing. (A) Unconfined compression and (B) Confined compression.



The unconfined compression test is the most commonly performed test to characterize NP replacement materials and enables valuable information relating to material mechanical properties be obtained. These include, but are not limited to, the compressive strength which can be calculated from the failure stress values from a stress–strain curve.

Despite being a direct parameter, considered to be relatively easy-to-measure, the compressive failure strength of various NP replacement materials has rarely been reported.^{32–35} This is due to several factors including the observation that in unconfined compression, weak and brittle materials (such as various hydrogels) tend to fail when exposed to near-physiological levels of compressive force.³⁴ For such mechanically weak materials, unconfined loading does not fully represent the conditions *in vivo* where in IVDs, NP is confined by the AF, and this confinement makes the brittle, catastrophic failure of the bulk material less likely to occur.³⁶ Although brittle failure/fragmentation of hydrogel implants and subsequent extrusion through AF incision defects can occur and has been reported by Durdag et al.,¹⁹ such evaluations would be more effectively performed through the use of cadaveric/spinal models.¹¹ For some synthetic polymeric hydrogels, samples often deform plastically in compression without fracture due to the highly connected gel/polymer network. Assessing compressive strength in hydrogels therefore remains a challenge and researchers are therefore more interested in assessing various modulus values to predict the clinical efficacy of hydrogels in application as NP replacements.

3.1.2 | Unconfined compression tests—Young's modulus

The Young's modulus/compressive modulus describes the ability of a material to resist elastic deformation upon being compressed. The greater the modulus, the stiffer the material and the harder to deform the bulk sample.³⁷ It can be obtained from the compressive stress–strain curve. Tangent modulus, which is the slope of the tangent line at one specific strain value, and secant modulus, which corresponds to the slope of the line connecting the point of zero strain to the deformation point at a given strains, are the most commonly used methods

for calculating the Young's modulus. Alternatively, Young's modulus may be calculated within the region of linear elastic deformation.³⁸ Recently, Ren et al. argued that the traditional tangent and secant methods introduce calculation errors and instead proposed the least-square method be implemented to simulate the loading curve. Following polynomial data fitting, the derivative of the fitted curve may be used to obtain Young's modulus values.³⁹

Hydrogels are the most popular class of polymer materials used for NP replacement/regeneration and for the vast majority of hydrogels, the stiffness increases with higher strain (strain-stiffening).^{40,41} As a result, defining a single Young's modulus value for hydrogel materials is not always feasible. The approximate axial strain level of intact physiological IVDs while walking corresponds to around 15%.⁴² In an early study, Boelen et al. proposed that an NP replacement material should withstand at least 30% compression without undergoing plastic deformation and catastrophic failure.³⁸ Therefore, most investigations aimed at fabricating NP implants have attempted to attain compressive modulus values within the strain range of 10%–30%. (Table S1).

Several additional factors need to be considered when evaluating single-cycle unconfined compression. Firstly, the typical loading rate most commonly employed is 100% strain/min, although slower (3% to 18% strain/min) loading conditions have also been reported.^{38,43,44} To mimic *in vivo* conditions, several studies have conducted compression tests when samples were immersed in water/PBS in order to prevent the sample from drying during the testing process. It is preferable for material testing to be conducted at 37°C as opposed to room temperature (25°C) since polymeric material properties are temperature-dependent and material testing at 37°C better recapitulates the microenvironmental temperature in native IVDs.⁴⁰ Control of sample temperature during compression testing often requires the use of custom-made setup configurations. As such, studies published by Cloyd et al. and Schmocker et al. have described the assembly of testing configurations which were simple in design yet capable of functioning as both a water bath (for temperature control) and a mount for optical cameras to monitor material deformation.^{45,46} Sample dimensions have also been reported to affect Young's moduli obtained from unconfined compression. In a series of studies, researchers have found stiffness values to be greater for wider and

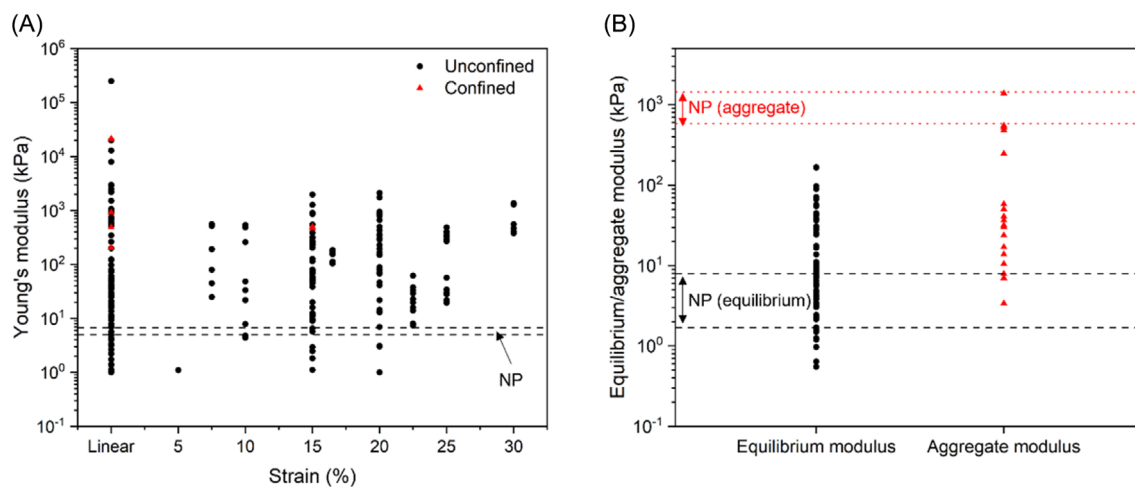


FIGURE 4 Plots of (A) Young's moduli and (B) equilibrium moduli and aggregate moduli collected from the literature (individual studies are listed in the Supplementary Material, Table S1). The range of moduli for native human NPs is shown as the gap between the dashed/dotted lines.^{45,51,52}

higher cylindrical-shaped samples, which may be due to the presence of greater cross-linking densities in larger samples.^{47–49} Although a wide range of sample dimensions have been used across studies, it is reasonable to suggest that conducting compression tests on disc-shaped materials with similar dimensions to native human NP (~20 mm diameter and ~10 mm height) remains ideal.⁵⁰

Young's modulus data from 50 published studies on NP replacement/regenerative materials was collected and provided in the supplementary material (Table S1) whilst an illustration of the literature findings is shown in Figure 4A. As depicted, a wide range of Young's modulus values have been reported (~5 orders of magnitude). Young's moduli for healthy native human NP was estimated by Umehara et al. to be between 5 and 6.7 kPa as determined using an indentation measurement approach.⁵¹ Through biomechanical characterization experiments and finite element methods (FEM), many researchers have proposed the ideal range of Young's moduli for NP replacement implants. From FEM, Meakin and Hukins proposed that in the case of a full-size implant, a material with a 3 MPa modulus would be most suited to match the stress distribution of an intact disc.¹⁵ A later study also confirmed this result, concluding that 1–4 MPa to be the optimal modulus range for NP replacement devices.¹⁷ In a subsequent study, Meakin and colleagues conducted experiments using polymers with varying degrees of material stiffnesses. They concluded that no significant inward bulging of AF was observed when solid implants with Young's moduli from 0.2 to 40 MPa replaced the native NP.⁵³ Joshi et al. also contributed to the prediction of the ideal NP implant Young's modulus. From two FEM studies, the authors first suggested that 30 kPa to 3 MPa be the ideal modulus for hydrogel NP implants.⁵⁴ Later, in a more comprehensive study, they found that only slight variations in the IVD compressive behavior were observed when implants with a modulus from 0.01 to 5 MPa were used. As expected, higher moduli (above 5 MPa) may lead to stress shielding for the surrounding AF.¹⁶ Drawing insights from all of the aforementioned investigations, it is reasonable to conclude that within a certain range, from around

native tissue modulus (10 kPa) to a value that prevents stress shielding and endplate sinking (5 MPa),¹⁶ there exists a large tolerance in the Young's modulus for NP replacement devices for ensuring the suppression of the abnormal inward bulging of the AF after NP removal. In addition, implant geometry and volumetric filling conditions (over-filled, line-to-line fit, and under-filled) also play significant roles in restoring the disc stiffness; line-to-line and over-filled conditions are more effective at restoring IVD loads to the intact level.¹⁶

3.1.3 | Unconfined compression tests—equilibrium's modulus

Apart from compressive modulus, additional considerations describing material mechanical properties may be obtained from unconfined compression tests. One such property is the equilibrium modulus which reflects the mechanical properties of the implant material in equilibrium conditions such as sitting or resting and may be measured from unconfined relaxation tests.⁵⁵ Such tests may be conducted in single-ramp or multi-ramp (incremental) loading conditions. For single-ramp conditions, a load is applied at a specific strain level (10%–20%) where the displacement is held for a long enough period for the material to achieve complete relaxation to equilibrium, typically 20 mins in the case of NP replacement implants.^{44,56} The stress and strain data at the end of the relaxation period can then be used to calculate the equilibrium moduli.

Multi-ramp incremental compression is an example of an unconfined compression test which is most commonly used to obtain equilibrium moduli. Cloyd et al. first adapted five-ramp compression with 5% strain increments at 5% strain/s.⁴⁵ Following each ramp cycle, the displacement was kept constant for a sufficient period for complete relaxation, and the strain increments were repeated to 25% strain. Three-ramp compression is also commonly implemented with 5% strain increments to achieve a final strain level of 15%.^{57–59} The complete relaxation time varies with materials, and is defined as

<0.001 kPa/s change in stress,⁵⁶ or <0.5 g change in reading in 10 min.⁵⁷ The equilibrium stress and strain data at the end of each ramp period/relaxation period can then be plotted to determine the equilibrium moduli. For the five-ramp compression, and in the case of a non-linear 'J-shaped' stress-strain response, the slope of the curve at 0% strain is termed the "toe-region modulus", and the slope at 20% strain is considered as the "linear-region modulus".⁴⁵ Using the five-ramp compression test, Cloyd et al. measured the equilibrium moduli for nondegenerate human NP and found values to range between 3.25 ± 1.56 kPa (toe modulus) and 5.39 ± 2.56 kPa (linear modulus).⁴⁵ Considering the requirement for achieving material stability, an ideal NP implant ought to have a stiffness (equilibrium modulus) that is similar to or greater than the native NP, and this criterion is well demonstrated in Figure 4B. A dense cluster of data points lies within the native NP range (black dashed lines), and a large proportion of the materials developed are stiffer than the human NP.

Another parameter which can be measured together with the equilibrium modulus is the Poisson's ratio. Poisson's ratio (ν) describes the material deformation in the direction perpendicular to the direction of the applied force and can be calculated as the ratio between the lateral strain (perpendicular to the compressive force) and axial strain (direction of the applied force): $\nu = -\left(\frac{\epsilon_L}{\epsilon_a}\right)$. In the context of designing NP implants, the Poisson's ratio is important since it is the lateral expansion of the NP which affects the load transfer in the disc and its interaction with the surrounding AF. The Poisson's ratio for nondegenerate human NP was also reported by Cloyd et al.⁴⁵ By optically capturing the change of lateral expansion using a digital camera at different strain levels, the Poisson's ratio of the human NP was calculated to be 0.62 ± 0.15 , suggesting the anisotropic and compressible nature of the NP due to fiber reinforcement and fluid flow under loading conditions.

3.1.4 | Unconfined compression tests—creep, relaxation, and fatigue tests

Creep and relaxation are two fundamental properties to consider when designing NP implants. Both are attributed to the viscoelastic properties of the implant materials. Creep describes material deformation under mechanical stress (how strain changes under constant stress). In natural IVD, creep occurs under load due to the flow of bodily fluids which causes human height loss during the day.⁴³ Usually, creep can be observed with samples which have been subjected to a static load.⁶⁰ However, the cumulative effect from cyclic loading can also lead to creep.⁴³ For the creep test, a tare load (usually 1 to 2 g) is applied to the sample, and the creep displacement is monitored until equilibrium is reached^{44,61}; equilibrium is defined as <10 μ m change in displacement in 10 min.⁶²

Following the creep test, single-ramp or multi-ramp stress relaxation tests are usually carried out. Stress-relaxation tests are important to investigate the time-dependent sensitivity to an external load (how stress changes under constant strain).⁶³ Under constant strain, due to

the intrinsic viscoelastic property, crosslinks within a hydrogel matrix unbind, allowing the hydrogel to flow, leading to a change in the stress state.⁶⁴ The same procedures used for measuring equilibrium moduli (i.e. single/multi-ramp unconfined compression), as discussed in the subsection above, can be used to determine relaxation. From the single/multi-ramp relaxation data, relaxation percentage can be calculated using the following formula: $\left(1 - \frac{\sigma_e}{\sigma_p}\right) \times 100\%$, where σ_p is the peak stress after the load has been applied to the sample and σ_e is the equilibrium stress at the end of the relaxation period of the ramp. Using this method, Cloyd et al. determined the percent relaxation of native human NP to be $34.23 \pm 11.3\%$.⁴⁵

The longevity of NP implants should be maximized in order to ensure long-term therapeutic success and material stability in patients. In addition to total material failure, one possible way for implants to lose functionality is through the reduction in height due to long-term loading conditions. The large number of loading cycles experienced by IVDs during daily activities leads to cumulative fatigue of the material which changes the relaxation behavior of hydrogel polymer chains. A reduction in hydrogel relaxation potential ultimately effects the creep behavior of the hydrogel and may lead to overall shape changes of the implant.⁴⁸ Fatigue testing is a time-consuming process which may require the mechanical testing system to continuously operate for several days. The authors speculate that this may explain why only a few studies report material properties after fatigue loading.^{11,27,39,42,43,48,60,65-67} With compressive loading frequencies below 10 Hz (most commonly 5 Hz), samples are compressed to around 15%–20% strain for up to 10 million cycles.^{42,43,48,60,66} It is worth noting that fatigue tests may also be performed in a confined manner.¹¹ Furthermore, in order to accurately evaluate the mechanical performance of NP implants researchers often conduct fatigue tests while embedding implants inside *ex vivo* spinal models such as bovine or porcine lumbar spine segments (see Section 3.3 *Tests in spinal models*).^{27,65,67} The change in mechanical properties of the motion segment during the testing process indicates the effectiveness of NP implants against cyclic fatigue loading. A NP implant with good fatigue resistance should help maintain the deformation behavior of the testing motion segment throughout the loading cycles.

3.1.5 | Confined compression tests—aggregate modulus and permeability

Confined compression tests (Figure 3B) are frequently performed due to the physiological relevance whereby the native NP experiences semi-confined loading *in vivo*.²⁵ From confined compression tests, aggregate modulus (H_A) and permeability coefficient are commonly obtained. By definition, the aggregate modulus measures the stiffness of the soft material at equilibrium when the flow of fluids has ceased. The smaller the aggregate modulus, the more the tissue/material deforms under a given load.⁶⁸ Aggregate modulus can be measured and calculated in a similar manner as that of the equilibrium modulus, as described in Section 3.1.3, but in a confined condition.^{69,70} Aggregate modulus can also be determined through its relationship with the

unconfined equilibrium modulus (E_{eq}) and Poisson's ratio (ν) via the following equation⁷¹: $H_A = \frac{E_{eq}(1-\nu)}{(1+\nu)(1-2\nu)}$. Aggregate moduli of NP implants from the literature are shown in Figure 4B. As expected, since the aggregate modulus includes the contribution of osmotic pressure due to swelling, the aggregate modulus values (red triangles) are generally higher than the equilibrium moduli obtained from unconfined compression (black dots). For nondegenerate human NP, the aggregate modulus was measured by Johannessen et al. to be 1010 ± 430 kPa.⁵² From the figure, most materials developed possess smaller aggregate moduli than the healthy native human NP.

Permeability, which measures the resistance of fluid flow through a porous material, reflects the rate at which the fluid exits the matrix and affects the compressive load response of the material. For a material with high permeability, fluid can easily flow out of the bulk matrix, and the equilibrium can be reached in a shorter time.⁶⁸ Hydraulic permeability (k_a) of a material can be obtained from the linear biphasic models after fitting the relaxation data from the confined compression^{72,73} ($k_a \sim 9 \times 10^{-16} \text{ m}^4 \text{ N}^{-1} \text{ s}^{-1}$ for healthy human NP⁵²). For biomaterials, the intrinsic permeability is closely related to the porosity and pore size of the scaffold.⁷⁴ Apart from being an important parameter in understanding the regulation of fluid flow, the permeability also reflects the ability of the matrix to transport nutrients.⁷⁴ From these considerations, it is ideal for the implant to have similar permeability as the native NP tissue. However, Chan et al. also argued that an enhanced permeability of the biomaterial might be desirable for tissue recovery due to promoted cellular growth and attachment.⁷⁵

3.2 | Rheology

Similar to many other soft tissues in the human body, the NP is viscoelastic, meaning that during deformation the NP shows both elastic (solid-like) and viscous (liquid-like) characteristics.³¹ Hydrogels are great candidates to mimic such properties due to their biphasic nature (solid network surrounded by an aqueous solution).^{20,76} To study the viscoelastic behavior of hydrogels, their rheological properties are commonly measured. From the dynamic rheological measurement (either in shear or compressive mode), a complex modulus can be obtained through the following formula:

$$G^* = G' + iG'' \text{ (shear) or } E^* = E' + iE'' \text{ (compressive),}$$

where G^* (E^*) is the complex shear (compressive) modulus, G' (E') is the storage/elastic shear (compressive) modulus and G'' (E'') is the loss/viscous shear (compressive) modulus. G' (E') represents the solid-like/elastic behavior, while G'' (E'') describes the liquid-like/viscous behavior of a material.⁷⁷

If the storage modulus is greater than the loss modulus, then the material behaves like a solid/gel. Contrastingly, if the loss modulus is greater than the storage modulus, then the material behaves like a liquid. The dynamic complex modulus indicates the total resistance of a material to deformation, and this is analogous to the overall stiffness of the material.⁷⁸ During testing of potential NP hydrogel implants, an

amplitude/stress sweep test is first conducted to determine the linear viscoelastic region of the test material. A frequency sweep within the viscoelastic region is often carried out thereafter. If one wants to observe the *in situ* gelation behavior of hydrogels, then a single-frequency oscillation-time sweep test may be performed to observe the change of G' and G'' as a function of time. The moment where G'' curve starts to exceed the G' curve can be defined as the gelation time of the hydrogel (Figure 5A),⁷⁹ which can provide useful information on the operation window in surgical scenarios. For NP implants, it is considered ideal for tests to be conducted at 37°C such as to recapitulate the physiological temperature of the human body.

In most cases, the moduli values change under different frequencies. Therefore, in this review, all hydrogel moduli values were collected at 10 rad s^{-1} (1.6 Hz) or 1 Hz, where the frequency-induced variation is negligible. A collection of obtained hydrogel moduli values from literature is illustrated in Figure 6. Iatridis et al. reported the mean complex shear modulus to be 11.3 kPa for nondegenerate human lumbar NP at 10 rad s^{-1} .^{31,80} From Figure 6, it can be seen that most investigated hydrogels show dynamic moduli lower than that of the native tissue. Although there are also hydrogels with extremely high moduli (10^4 kPa), the injectability of such hydrogels are compromised.³⁸ Clinical studies have shown that NuCore® Injectable Nucleus hydrogel (manufactured by Spine Wave, Inc., Shelton, CT, USA) with a 26 kPa complex shear modulus was able to greatly restore disc height clinically after a 2-year follow-up period.⁸² In addition to the shear rheology, from compressive dynamic mechanical analysis (DMA), dynamic compressive moduli can be obtained. Leahy et al. reported the complex compressive modulus for sheep NP to range from 20 to 130 kPa.⁸¹ From the literature data, the reported dynamic compressive moduli are centered around this range (Figure 6), although the situation may be slightly different for human tissues.

An additional parameter obtained from the dynamic rheological measurement is the phase shift angle which is measured using the following formula:

$$\delta = \tan^{-1}\left(\frac{G''}{G'}\right) \text{ or } \tan^{-1}\left(\frac{E''}{E'}\right),$$

The phase shift angle measures the internal dissipation of the hydrogel. For a perfectly elastic material (solid), the phase shift angle value equals 0, while for a perfect fluid, no energy can be stored, and the stress and strain are 90° out of phase.⁶³ Iatridis et al. measured the phase shift angle of human NP across a range of frequencies (1 rad s^{-1} to 100 rad s^{-1}) and found that the NP showed predominantly elastic behavior, with G' consistently being greater than G'' and δ being consistently below that of 45°. At 10 rad s^{-1} , the human NP has a phase shift angle of $24 \pm 5^\circ$.³¹ From the compressive dynamic mechanical analysis, sheep NP also revealed a similar mean phase shift angle of 18°.⁸¹ Therefore, it is important to deduce if soft NP hydrogel implants possess phase angles below that of 45° at physiologically relevant frequencies.

Utilising injectable materials, such as hydrogels, is ideal for minimally invasive surgical implantation of restorative biomaterials.

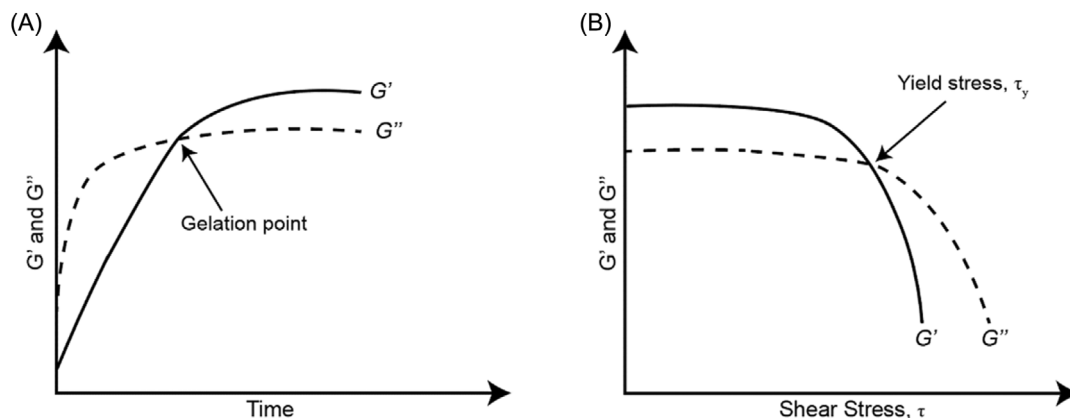


FIGURE 5 Rheological measurements to obtain (A) the gelation point of the *in situ* gelling hydrogels and (B) the yield stress of shear-thinning injectable hydrogels.

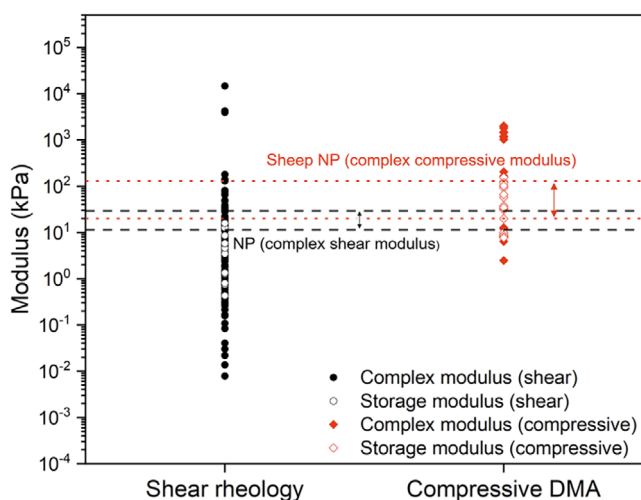


FIGURE 6 Plot of complex moduli and storage moduli collected from literature (individual studies are listed in the Supplementary Material, Table S1). All moduli values were obtained under the frequency of 10 rads⁻¹ (1.6 Hz) or 1 Hz. The range of complex shear moduli for native human NPs and complex compressive moduli are shown as the gaps between the black dashed and red dotted lines, respectively.^{31,80,81}

Some hydrogel formulations have the ability to be injected while in a liquid phase, followed by *in situ* crosslinking to facilitate curing.^{58,79} For such materials, the mechanical properties following crosslinking are of greater significance. In other cases, hydrogels are crosslinked prior to implantation where the injectability is then attributed to their shear-thinning (pseudo-plastic) characteristic of the gel.^{78,83–86} As the shear rate increases, the viscosity of the hydrogel decreases. When the viscosity decreases to a point where the gel can flow like a liquid ($G'' > G'$), it can be considered injectable. Many studies demonstrate a decrease in viscosity with higher shear rates to highlight the shear-thinning properties and the injectability of hydrogel formulations. However, it should be noted that for these designs, both the mechanical properties before and after the injection through a needle/catheter

should be measured. Studies have shown that the injection of material leads to a drop in hydrogel storage modulus, possibly due to the disruption of polymeric networks incurred by the shear force created during the injection process.^{83,87}

For shear-thinning hydrogels, the additional rheological parameter that can help determine the injectability and the stability of hydrogel NP implants is the yield stress. From the stress sweep test, the yield stress can be determined by the crossover of the storage modulus (G') and loss modulus (G'') curves (Figure 5B).⁸⁸ Although few studies have discussed this, the yield stress can help quantify the injectability of the hydrogel in assessing how much stress is required to make the gel “flow”. For cell-encapsulated gels, the shear-thinning property and a low yield stress helps protect the cells from physical stress, thus improving their overall survivability.⁸⁹ Furthermore, these parameters can may also be used to describe the mechanical stability of hydrogels.^{79,90} If the stress experienced by the hydrogel is greater than that of the yield stress, the risk of the viscoelastic gel starting to “flow” and being extruded out of the AF incision (expulsion) will also be greater.

3.3 | Tests in spinal models

In addition to testing biomaterials by themselves, researchers have made use of various spinal models to conduct *ex vivo* biomechanical tests. These models involve the use of either cadaveric lumbar spines from donors,^{11,60,91,92} or functional spinal units from animals (bovine,^{46,59,67,93–95} porcine,^{47,96} goats,⁹⁷ rabbits,⁹⁸ and rats⁹⁹). The major purpose of these tests is to determine whether the implanted material can help restore the biomechanics to that of the normal spine. A simple method for performing such *ex vivo* tests is by comparing the compressive stiffness of the functional spinal units among the intact, after denucleation, and after implantation groups. These techniques are well established and documented through several research efforts.^{59,60,67,91,93,96,98} A functional NP implant should help restore the stiffness of the implanted specimen to the intact level.^{60,91} In addition, after cyclic compression, the dimension of the samples can

TABLE 2 Techniques to characterize the mechanical properties of NP implants.

Mechanical testing	Information obtained for the biomaterials developed	Nondegenerate human NP data (if applicable)
Unconfined compression	Young's modulus	5.00 to 6.70 kPa ⁵¹
	Equilibrium modulus	3.25 ± 1.56 kPa (Toe region) ⁴⁵
		5.39 ± 2.56 kPa (Linear region) ⁴⁵
	Poisson's ratio	0.62 ± 0.15 ⁴⁵
	Percent relaxation	34.23 ± 11.3% ⁴⁵
Fatigue resistance	-	
Confined compression	Aggregate modulus	1010 ± 430 kPa ⁵²
	Permeability ($\times 10^{-16}$)	9.00 ± 4.25 $m^4 N^{-1} s^{-1}$ ⁵²
	Fatigue resistance	-
Rheology	Complex shear modulus	11.3 ± 17.9 kPa (at 10 $rad s^{-1}$) ^{31,80}
	Complex compressive modulus	20–130 kPa (Sheep NP) ⁸¹
	Phase shift angle	24 ± 5 ° (at 10 $rad s^{-1}$) ^{31,80}
	Gelation time/yield stress (injectable gels)	-
Spinal models	Biomechanics restoration	-
	Disc height restoration	-
	Implant extrusion	-
	Fatigue resistance	-

be measured to see if the reduction in IVD height can be rescued.^{46,93} With an injectable fibrin-hyaluronan hydrogel, Li et al. showed that although the disc height dropped after the dynamic loading, which corresponded to activities during the day, the disc height was restored to the intact IVD level after overnight free swelling, which was analogous to the resting period.⁹³ Therefore, whether the IVD height can be recovered after loading should be investigated. In addition, parameters which reflect the restoration of additional mechanical properties of the IVDs, such as range of motion (ROM) and neutral zone (NZ) length, can be determined.^{14,59,65,94,96} As discussed previously, spinal models are also useful in fatigue tests to evaluate the durability of NP implants.^{27,65,67}

A common clinical complication for NP implants is the extrusion of the replacement material. Spinal models can also be used to evaluate the biomaterial to avoid unwanted extrusion. Following implantation, the motion segments can be tested to failure in various modes (compression, anterior flexion, and lateral bending in the direction opposite to the annular incision). The failure can be defined as endplate fracture, annulus rupture, ligament failure, lateral facet fracture, or significant implant protrusion.^{11,65,67} The failure strength/moments can then be compared to those of intact samples, and more

importantly, the extrusion of the implant can be observed.¹¹ From the load–displacement curves, Lin et al. reported subsidence-to-failure (the displacement prior to the failure point) and work-to-failure (area under the load–displacement curve before failure point), which were valuable for comparing the axial displacement and energy needed for the construct to fail. Importantly, it was suggested by Wilke et al. that these experiments should be carried out at room temperature, and the test duration should not exceed 20 hours to prevent the degradation and property changes in specimen.¹⁰⁰

Table 2 summarizes the above-mentioned characterization techniques and important information which can be obtained therefrom. Published data on native NP characteristics is included as reference.

3.4 | Post-mechanical testing: biological evaluations

When designing implantable biomaterials, biological properties cannot be ignored, both from the functionality and safety perspectives.¹⁰¹ Information obtained from various *in vitro* and *in vivo* experiments were collected and tabulated in Table S2.

As a starting point, most *in vitro* experiments assess the cytotoxicity of biomaterials through conducting cell viability assays. As shown in Figure 7A, NP cells are the most commonly utilized cell type for conducting biological assessments of potential NP implant biomaterials. Various NP cells isolated from animal discs (bovine, porcine, goat, rabbit, and rat) are commonly used in *in vitro* experiments. However, due to a lack of donor availability, only a few studies have conducted cytotoxicity tests directly on human NP cells isolated from human intervertebral discs^{102–105}; among all sources of NP cells, bovine NP cells are the most frequently used. Commonly employed *in vitro* assays include live/dead staining, metabolic activity (MTT), and cytotoxicity/proliferation (CCK-8) assays. In some cases, the neutral red uptake assay is used to evaluate cell viability.¹⁰⁶ For further confirmation of cell proliferation and morphology, the evaluation of collagen type-2 and aggrecan concentrations⁶³ or simply the detection of staining signals (absorbance) of the cells may be performed.^{47,75,107} Following cell viability and cytotoxicity assessments, it is crucial to visualize whether the cells adhere to the material surface or infiltrate into the material. Toluidine blue staining,⁹³ bioluminescent imaging by D-luciferin,¹⁰⁸ DAPI staining,¹⁰⁹ EdU assay,¹¹⁰ and the use of GFP-tagged cells¹¹¹ may all be utilized to observe cell distribution and localization.

While preliminary confirmation of material biocompatibility via *in vitro* assays is crucial, these assays often do not provide relevant information for what can be expected in clinical applications. Henceforth, biomaterial performance in *in vivo* animal models is fundamental to predict actual outcomes when implanted in human recipients. In most animal models, cellular implants incorporate NP cells or stromal cells for encapsulation and subsequent implantation (Table S2). Rats are most commonly used for *in vivo* experiments, followed by rabbits and mice (Figure 7B). Biomaterials may be implanted subcutaneously in small animals to assess the occurrence of inflammation when

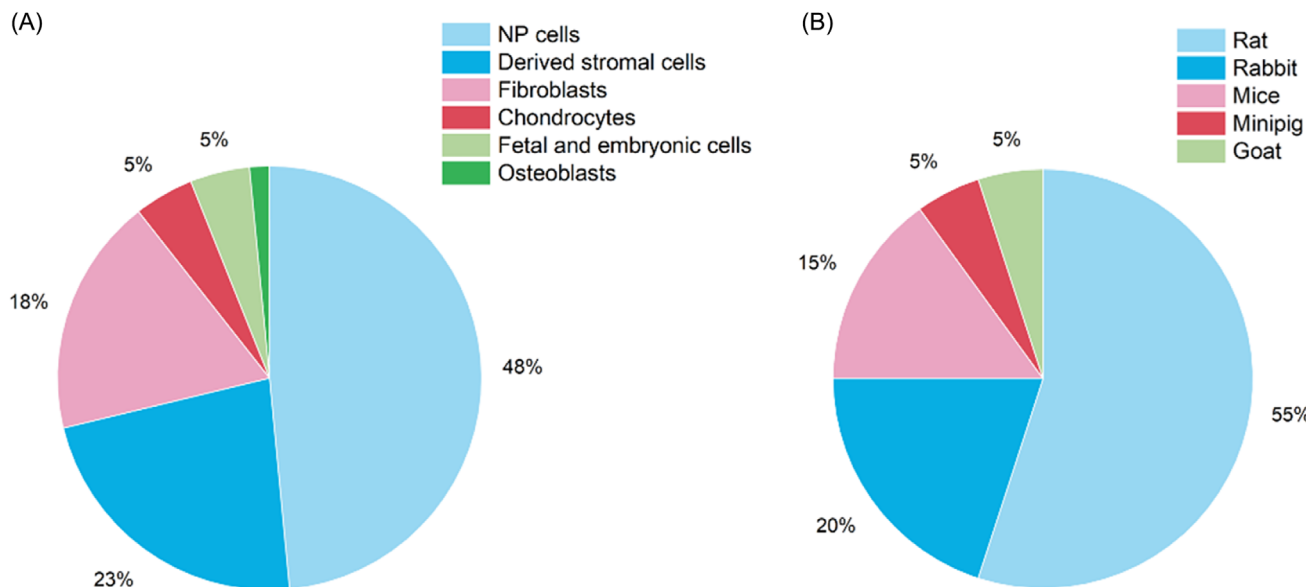


FIGURE 7 (A) Cell populations used in *in vitro* and (B) *in vivo* animal models implemented to evaluate NP implants. Data and references illustrated in Table S2.

analyzing the blood biochemistry of the animal. Hematoxylin and eosin (H&E) staining on sectioned tissues may be performed to determine whether biomaterial implants induce an inflammatory response.^{85,107} To evaluate the performance of the implant in replacing the NP, an annular puncture model of IVD degeneration may be used on either rat tails or rabbit IVDs^{102,111}; few studies have performed *in vivo* implantation in the IVDs of large animals such as minipigs or goats.^{107,112} Post-implantation, detection of collagen type-2, GAGs, SOX-9, and aggrecan by histochemical staining and/or genetic analysis is required to assess whether there are alterations in the phenotypes of the implanted cells (Table S2).

4 | CURRENT BIOMATERIALS DESIGNS: HOW TO MIMIC?

A variety of materials have been utilized to develop NP replacement/regeneration implants based on various design criteria. The primary consideration, as the previously discussed, is designing a material with optimal mechanical properties to ensure that the material is capable of performing its restorative function. Apart from material mechanical properties, the restoration of IVD biomechanics also depends on the filling condition of the implant. An over-filling or line-to-line filling of the nucleus cavity leads to a better restoration effect and avoids implant migration.^{16,113} Therefore, from this perspective, the material needs to be expandable or injectable. For achieving minimally invasive surgical procedures, formulating injectable materials which may be directly delivered to the repair site is desirable.¹¹⁴ Depending on the intended application (either a permanent substitute or a cell-incorporated and degradable implant for effective tissue regeneration) the degradation of the material should be specifically tailored.¹¹⁵ For permanent synthetic

implants, significant degradation should not occur in the long-term. For degradable implants, the degradation rate should match the rate of tissue regeneration.¹¹⁶ As a common criterion for all biomedical materials, biological properties such as biocompatibility and bioactivity are critical.

Currently, hydrogel-based materials are considered promising candidates for NP implants and are the focus of the majority of research within the field. In addition to having similar viscoelastic properties as the native NP tissue, hydrogels are easy to apply to IVDs in clinical situations. Hydrogels are well known for their water-absorbing properties, providing them the ability to swell. One strategy to accurately apply hydrogels to the NP cavity is by introducing dried (dehydrated) hydrogels which can be rolled and inserted into the cavity directly. Following implantation, subsequent hydrogel swelling *in situ* can help fully fill the cavity and provide enough pressure to restore physiologically relevant biomechanics.^{11,38} It is worth mentioning that in this case the mechanical properties of hydrogels can be affected by the dehydration history. As dehydration levels increase, compressive moduli of the hydrogel after rehydration also increases, which may be due to the higher cross-linking density upon drying.⁴²

Apart from the dehydration-rehydration approach, much attention has been given to the development of hydrogels capable of undergoing *in situ* curing (polymerization). Hydrogel curing mechanisms can be enzymatic,¹¹⁷ ionic,⁵⁷ or covalent,⁴⁹ and the leakage of the material before crosslinking should be minimized to avoid any adverse effects to surrounding tissues. Pre-gelled solutions with high viscosities or shear-thinning properties are ideal for precise delivery of hydrogel materials from a syringe. Researchers have also been focusing on thermoresponsive^{27,46,79,118,119} and photo-crosslinkable hydrogels.^{46,57,58,109,120-124} One major advantage for thermoresponsive hydrogels such as poly(*N*-isopropylacrylamide) (PNIPAAm) is that the gelation occurs due to a phase transition process, which avoids

the exothermic polymerization reaction that raises the surrounding temperature.¹¹⁸ For photo-crosslinkable hydrogels which require ultra-violet (UV) induced polymerization, prolonged UV exposure and introduction of potentially toxic photoinitiators often negatively effects cell viability.⁵⁸ For hydrogels formed outside the body, such as the poly(vinyl alcohol) (PVA)–poly(vinyl pyrrolidone) (PVP) hydrogel made via freezing–thawing, one strategy to enable them be injectable is by molding them into strings and injecting the strings into the NP cavity.¹²⁵ However, for this approach, making a cohesive implant is challenging and due to the lack of integrated bulk construct, the fragmentation of thin hydrogel filaments and the subsequent extrusion from the AF incision may be problematic.¹⁹ A future direction for using hydrogel NP replacement is the development of self-healable implants. Pérez-San Vicente et al. demonstrated that an injectable and self-healable dynamic hydrogel based on gold(I)-thiolate/disulfide (Au – S/SS) exchange could recover its mechanical properties post-loading.⁹⁴ Furthermore, unlike traditional covalently bonded hydrogels, the dynamic moduli of self-healable hydrogels did not change following extrusion from a syringe.^{83,87,94} This is helpful to avoid hydrogel fragmentation inside the body and the catastrophic expulsion of the nucleus implants. Despite the promising properties from a mechanics perspective, the *in vivo* biocompatibility of such materials needs to be investigated. Self-healing hydrogels such as PVA hydrogels based on noncovalent interactions (hydrogen bonds),¹²⁶ have been revealed to be nontoxic in nature. However, their self-healing performance is greatly deteriorated in submerged (body fluid) environments.^{127,128} Therefore, an injectable, biocompatible hydrogel with rapid under-water self-healing abilities is needed.

Apart from hydrogels, several synthetic materials have demonstrated potential application as NP implants. In an early study, researchers used polycarbonate urethane (PCU) and applied it to the NP cavity as a memory coiling spiral. A unique property of PCU is that it allows maximal filling of the intradiscal space; however, the damping property (the ability to dissipate elastic strain energy during mechanical vibration) of the native NP could not be mimicked.¹²⁹ Recently, Shaha et al. demonstrated that polydomain elastomers based on liquid crystals exhibit a near-identical compressive behavior to the native NP. Interestingly, liquid crystal elastomers also demonstrate high energy dissipation which match the phase shift angle to that of the native NP tissue.⁹² Porous titanium has also been investigated as NP implants.^{39,65,130} Although porous metal implants have shown excellent biocompatibility and physiologically relevant mechanical properties, debris formation and the fracture of metal filaments under various conditions still need further comprehensive investigation.³⁹ One novel design is the use of a balloon NP replacement systems. In a recent study by Lee et al., a balloon-like implant comprising of a polyurethane (PU) jacket and a micro-valve was generated. Following insertion of the flattened PU jacket into the NP cavity, a fluid was injected through the valve to achieve inflation.¹¹³ Such a jacket-valve design can avoid implant migration and expulsion, and at the same time, since the injection of fluid is manually controlled, the applied pressure can be accurately modulated. Furthermore, the injectable fluid/hydrogel material may be fine-tuned to adjust the overall mechanical characteristics of the construct. The combination of inflatable balloons with various injectable fluid/hydrogels may be an exciting direction to investigate.

However, additional tests need to be conducted to assess the durability of the outer jacket and possible leakage of the inner filling in the long-term.

5 | FUTURE PERSPECTIVES: ARE WE THERE YET?

An ideal NP replacement material should fulfill several requirements including restoration of the IVD height, regulation of the intradiscal pressure, and enable normal range of motion of the spine. Unfortunately, no such material has proven significant clinical success in achieving these requirements. A major limitation which needs to be addressed is that under pressure, extrusion of implant materials often occurs, leading to device failure and additional complications.¹³¹ To overcome this challenge, comprehensive mechanical characterizations need to be performed. Quantifiable techniques including compressive and rheological measurements on the material itself are necessary. Tests in spinal models (either human cadaveric or animal specimens) to evaluate the restoration performance, fatigue resistance, and risk of material extrusion, are also crucial. Alternatively, bioreactor systems can be used to recapitulate physiological conditions.⁴⁶ Most importantly, dynamic loading should be induced based on physiologically relevant loading conditions (shown in Table 1); harsh testing conditions may indicate the effectiveness and intactness of the implant *in vivo*.

From a material selection perspective, among all candidate materials, hydrogel-based systems appear to be the most promising option considering their soft-tissue mimicking mechanical properties, biodegradability, and ease of surgical injection. However, unlike native tissues, traditional acellular hydrogels lack the ability to remodel the matrix, leading to deteriorated mechanical properties after a fracture or in the long-term. Developing injectable and self-healable hydrogels may be a direction to solve this, and further efforts are required to achieve a biocompatible hydrogel formulation which is both mechanically strong and rapidly self-healable. Developing cell-incorporated hydrogel implants is more challenging compared to their acellular counterparts, since the cellular activities affect the degradation of the hydrogel matrix, which in turn alters the mechanical properties of the soft implant. In this case, finding the balance between the rate of hydrogel degradation and that of neo-NP tissue formation is required. Furthermore, a stiff hydrogel may negatively affect injectability and due to a high crosslinking density, cell ingrowth and migration may be hindered.¹³² Apart from pure hydrogels, composite systems such as the balloon jacket filled with NP-tissue mimicking hydrogels may also be comprehensively studied in the future. Following inflation of the balloon, the outer jacket prevents the extrusion of the implant while at the same time also protects the hydrogel from making contact with body fluids which would otherwise degrade the hydrogel matrix.

The concern over extrusion of NP implant material may also be addressed by including an AF closure device. Recently, Zengerle et al. demonstrated that by combining the use of an NP implant with the closure of an AF defect, normal spinal biomechanics could be restored, and no signs of NP implant extrusion was observed in spinal

models.¹³¹ Since various biomaterials have been developed for AF closure, it may be worth attempting to combine such devices alongside existing NP implant materials to best achieve overall restorative performance.¹³³⁻¹³⁵

6 | CONCLUSION

The use of NP implants has been proposed as a promising approach for treating degenerated IVDs. For these implants to be functional, comprehensive mechanical characterization is required to avoid complications such as implant fragmentation, and expulsion. In addition, rheological measurements are critical to determine the viscoelastic properties and the injectability of hydrogel materials. Since the loading condition in IVDs is complex, biomechanical testing systems based on spinal motion segments should also be employed to mimic *in vivo* conditions. When designing NP implants, preventing device extrusion and re-herniation should be the top priority. With the emergence of increasingly advanced material designs and formulations, unified characterization procedures are ideal for proof of superiority when novel materials are compared with existing devices. Through reviewing the commonly used experimental protocols from published literature, this review serves as a reference material for the future development of NP replacement/regeneration materials.

ACKNOWLEDGMENTS

This work is supported by the University of Hong Kong Seed Fund for Translational and Applied Research (104006073), Sanming Project of Medicine in Shenzhen “Team of Excellence in Spinal Deformities and Spinal Degeneration” (SZSM201612055) and HKU-SZH Fund for Shenzhen Key Medical Discipline (SZXK2020084).

DATA AVAILABILITY STATEMENT

The data that support the findings of this study are available from the corresponding author upon reasonable request.

ORCID

Zhuoqi Lucas Li  <https://orcid.org/0009-0009-6649-3593>

Sandra Hiu-Tung Wan  <https://orcid.org/0000-0002-7974-5421>

Kelvin Wai-Kwok Yeung  <https://orcid.org/0000-0003-0887-088X>

Kenneth Man-Chee Cheung  <https://orcid.org/0000-0001-8304-0419>

REFERENCES

- Cheung JPY, Kuang X, Lai MKL, et al. Learning-based fully automated prediction of lumbar disc degeneration progression with specified clinical parameters and preliminary validation. *Eur Spine J*. 2021; 31:1960-1968.
- Mok FPS, Samartzis D, Karppinen J, Fong DYT, Luk KDK, Cheung KMC. Modic changes of the lumbar spine: prevalence, risk factors, and association with disc degeneration and low back pain in a large-scale population-based cohort. *Spine J*. 2016;16(1):32-41.
- Humzah MD, Soames RW. Human intervertebral disc: structure and function. *Anat Rec*. 1988;220(4):337-356.
- Yang F, Leung VYL, Luk KDK, Chan D, Cheung KMC. Injury-induced sequential transformation of notochordal nucleus pulposus to chondrogenic and fibrocartilaginous phenotype in the mouse. *J Pathol*. 2009;218(1):113-121.
- Tendulkar G, Chen T, Ehnert S, Kaps HP, Nüssler AK. Intervertebral Disc Nucleus Repair: Hype or Hope? *Int J Mol Sci*. 2019;20(15):3622.
- Urban JPG, Roberts S. Degeneration of the intervertebral disc. *Arthritis Res Ther*. 2003;5(3):120-130.
- Zhang Y, Drapeau S, An HS, Markova D, Lenart BA, Anderson DG. Histological features of the degenerating intervertebral disc in a goat disc-injury model. *Spine*. 2011;36(19):1519-1527.
- Zhu Q, Gao X, Gu W. Temporal changes of mechanical signals and extracellular composition in human intervertebral disc during degenerative progression. *J Biomech*. 2014;47(15):3734-3743.
- Risbud MV, Shapiro IM. Role of cytokines in intervertebral disc degeneration: pain and disc content. *Nat Rev Rheumatol*. 2014;10(1):44-56.
- Eyholzer C, Borges de Couraça A, Duc F, et al. Biocomposite hydrogels with carboxymethylated, nanofibrillated cellulose powder for replacement of the nucleus pulposus. *Biomacromolecules*. 2011; 12(5):1419-1427.
- Bertagnoli R, Sabatino CT, Edwards JT, Gontarz GA, Prewett A, Parsons JR. Mechanical testing of a novel hydrogel nucleus replacement implant. *Spine J*. 2005;5(6):672-681.
- Sun Y, Leung VY, Cheung KM. Clinical trials of intervertebral disc regeneration: current status and future developments. *Int Orthop*. 2019;43(4):1003-1010.
- Goel VK, Nishiyama K, Weinstein JN, Liu YK. Mechanical Properties of Lumbar Spinal Motion Segments as Affected by Partial Disc Removal. *Spine*. 1986;11(10):1008-1012.
- Wilke HJ, Kavanagh S, Neller S, Haid C, Claes LE. Effect of a prosthetic disc nucleus on the mobility and disc height of the L4-5 intervertebral disc postnucleotomy. *J Neurosurg*. 2001;95(2 Suppl):208-214.
- Meakin JR. Replacing the nucleus pulposus of the intervertebral disk: prediction of suitable properties of a replacement material using finite element analysis. *J Mater Sci Mater Med*. 2001;12(3):207-213.
- Joshi A, Massey CJ, Karduna A, Vresilovic E, Marcolongo M. The effect of nucleus implant parameters on the compressive mechanics of the lumbar intervertebral disc: a finite element study. *J Biomed Mater Res B Appl Biomater*. 2009;90(2):596-607.
- Rundell SA, Guerin HL, Auerbach JD, Kurtz SM. Effect of nucleus replacement device properties on lumbar spine mechanics. *Spine (Phila, Pa 1976)*. 2009;34(19):2022-2032.
- Wilke H-J, Heuer F, Neidlinger-Wilke C, Claes L. Is a collagen scaffold for a tissue engineered nucleus replacement capable of restoring disc height and stability in an animal model? *Eur Spine J*. 2006; 15(3):433-438.
- Durdag E, Ayden O, Albayrak S, Atci IB, Armagan E. Fragmentation to epidural space: first documented complication of Gelstix(TM.). *Turk Neurosurg*. 2014;24(4):602-605.
- Heo M, Park S. Biphasic Properties of PVAH (Polyvinyl Alcohol Hydrogel) Reflecting Biomechanical Behavior of the Nucleus Pulposus of the Human Intervertebral Disc. *Materials (Basel)*. 2022;15(3):1125.
- Liu Y, Gao GM, Yang KY, Nong LM. Construction of tissue-engineered nucleus pulposus by stimulation with periodic mechanical stress and BMP-2. *iScience*. 2022;25:104405.
- Azartash-Namin K, Azartash-Namin Z, Williams SA, Tran K, Khandaker M. Mechanical effectiveness of polyvinyl alcohol/polyvinyl pyrrolidone (PVA/PVP) as an intervertebral disc polymer. In ASME International Mechanical Engineering Congress and Exposition, Proceedings (IMECE). 2013.
- Pimenta L, Marchi L, Coutinho E, Oliveira L. Lessons Learned After 9 Years' Clinical Experience with 3 Different Nucleus Replacement Devices. *Sem Spine Surg*. 2012;24(1):43-47.

24. Newell N, Carpanen D, Evans JH, Percy MJ, Masouros SD. Mechanical Function of the Nucleus Pulposus of the Intervertebral Disc Under High Rates of Loading. *Spine*. 2019;44(15):1035-1041.
25. Vogel A, Pioletti DP. Damping properties of the nucleus pulposus. *Clin Biomech (Bristol, Avon)*. 2012;27(9):861-865.
26. Winn HR. *Youmans and Winn Neurological Surgery*. Elsevier Health Sciences; 2022.
27. Balkovec C, Vernengo J, McGill SM. The use of a novel injectable hydrogel nucleus pulposus replacement in restoring the mechanical properties of cyclically fatigued porcine intervertebral discs. *J Biomech Eng*. 2013;135(6):61004-61005.
28. Huang J, Yan H, Jian F, Wang X, Li H. Numerical analysis of the influence of nucleus pulposus removal on the biomechanical behavior of a lumbar motion segment. *Comput Methods Biomech Biomed Engin*. 2015;18(14):1516-1524.
29. Wilke HJ, Neef P, Caimi M, Hoogland T, Claes LE. New In Vivo Measurements of Pressures in the Intervertebral Disc in Daily Life. *Spine*. 1999;24(8):755-762.
30. Kim J, Yang SJ, Kim H, et al. Effect of shear force on intervertebral disc (IVD) degeneration: an in vivo rat study. *Ann Biomed Eng*. 2012; 40(9):1996-2004.
31. Iatridis JC, Setton LA, Weidenbaum M, Mow VC. The viscoelastic behavior of the non-degenerate human lumbar nucleus pulposus in shear. *J Biomech*. 1997;30(10):1005-1013.
32. Khandaker M, Kotturi H, Proghi H, et al. In vitro and in vivo effect of polycaprolactone nanofiber coating on polyethylene glycol diacrylate scaffolds for intervertebral disc repair. *Biomed Mater*. 2021;16(4): 45024.
33. Huang Y, Zhang B, Xu G, Hao W. Swelling behaviours and mechanical properties of silk fibroin-polyurethane composite hydrogels. *Compos Sci Technol*. 2013;84:15-22.
34. Beattie W, Bay B. Hydrogel composite as a nucleus pulposus replacement designed to resist extrusion while maintaining functional material properties. ASME International Mechanical Engineering Congress and Exposition, Proceedings (IMECE). 2010.
35. Park SH, Cho H, Gil ES, Mandal BB, Min BH, Kaplan DL. Silk-fibrin/hyaluronic acid composite gels for nucleus pulposus tissue regeneration. *Tissue Eng A*. 2011;17(23-24):2999-3009.
36. Abdul Rahman MZA, Ahmad Zaidi AM, Abdul Rahman I. Analysis of Comparison between Unconfined and Confined Condition of Foamed Concrete Under Uni-Axial Compressive Load. *Am J Eng Appl Sci*. 2010;3(1):68-72.
37. Callister WD, Rethwisch DG. *Materials Science and Engineering: an Introduction*. Vol 9. Wiley; 2018.
38. Boelen EJ, van Hooy-Corstjens CS, Bulstra SK, van Ooij A, van Rhijn LW, Koole LH. Intrinsically radiopaque hydrogels for nucleus pulposus replacement. *Biomaterials*. 2005;26(33):6674-6683.
39. Ren ZY, Huang J, Bai H, Jin R, Xu F, Xu J. Potential application of entangled porous titanium alloy metal rubber in artificial lumbar disc Prostheses. *J Bionic Eng*. 2021;18(3):584-599.
40. Jaspers M, Dennison M, Mabesoone MFJ, MacKintosh FC, Rowan AE, Kouwer PHJ. Ultra-responsive soft matter for strain-stiffening hydrogels. *Nat Commun*. 2014;5(1):5808.
41. Ma Y, Feng X, Rogers JA, Huang Y, Zhang Y. Design and application of 'J-shaped' stress-strain behavior in stretchable electronics: a review. *Lab Chip*. 2017;17(10):1689-1704.
42. Thomas J, Shuen A, Lowman A, Marcolongo M. The effect of fatigue on associating hydrogels for nucleus pulposus replacement. Proceedings of the IEEE Annual Northeast Bioengineering Conference (NEBEC). 2003.
43. Boelen EJ, Koole LH, van Rhijn LW, van Hooy-Corstjens CS. Towards a functional radiopaque hydrogel for nucleus pulposus replacement. *J Biomed Mater Res B Appl Biomater*. 2007;83(2): 440-450.
44. Kim DH, Martin JT, Elliott DM, Smith LJ, Mauck RL. Phenotypic stability, matrix elaboration and functional maturation of nucleus pulposus cells encapsulated in photocrosslinkable hyaluronic acid hydrogels. *Acta Biomater*. 2015;12:21-29.
45. Cloyd JM, Malhotra NR, Weng L, Chen W, Mauck RL, Elliott DM. Material properties in unconfined compression of human nucleus pulposus, injectable hyaluronic acid-based hydrogels and tissue engineering scaffolds. *Eur Spine J*. 2007;16(11):1892-1898.
46. Schmocker A, Khoushabi A, Frauchiger DA, et al. A photopolymerized composite hydrogel and surgical implanting tool for a nucleus pulposus replacement. *Biomaterials*. 2016;88:110-119.
47. Bhunia BK, Mandal BB. Exploring gelation and physicochemical behavior of in situ bioresponsive silk hydrogels for disc degeneration therapy. *ACS Biomater Sci Eng*. 2019;5(2):870-886.
48. Hu J, Lu Y, Cai L, et al. Functional compressive mechanics and tissue biocompatibility of an injectable SF/PU hydrogel for nucleus pulposus replacement. *Sci Rep*. 2017;7(1):2347.
49. Hu J, Chen B, Guo F, et al. Injectable silk fibroin/polyurethane composite hydrogel for nucleus pulposus replacement. *J Mater Sci Mater Med*. 2012;23(3):711-722.
50. Zhong W, Driscoll SJ, Wu M, et al. In vivo morphological features of human lumbar discs. *Medicine*. 2014;93(28):e333.
51. Umehara S, Tadano S, Abumi K, Katagiri K, Kaneda K, Ukai T. Effects of degeneration on the elastic modulus distribution in the lumbar intervertebral disc. *Spine*. 1996;21(7):811-819.
52. Johannessen W, Elliott DM. Effects of degeneration on the biphasic material properties of human nucleus pulposus in confined compression. *Spine*. 2005;30(24):E724-E729.
53. Meakin JR, Reid JE, Hukins DW. Replacing the nucleus pulposus of the intervertebral disc. *Clin Biomech (Bristol, Avon)*. 2001;16(7):560-565.
54. Joshi A, Karduna A, Marcolongo M. The effect of nucleus implant modulus on the mechanical behavior of lumbar functional spinal unit: A finite element study. Proceedings of the IEEE Annual Northeast Bioengineering Conference (NEBEC). 2003.
55. Lang G, Obri K, Saravi B, et al. Architecture-promoted biomechanical performance-tuning of tissue-engineered constructs for biological intervertebral disc replacement. *Materials (Basel)*. 2021;14(10):2692.
56. Mercuri JJ, Gill SS, Simionescu DT. Novel tissue-derived biomimetic scaffold for regenerating the human nucleus pulposus. *J Biomed Mater Res A*. 2011;96(2):422-435.
57. Chou AI, Akintoye SO, Nicoll SB. Photo-crosslinked alginate hydrogels support enhanced matrix accumulation by nucleus pulposus cells in vivo. *Osteoarthritis Cartil*. 2009;17(10):1377-1384.
58. Chou AI, Nicoll SB. Characterization of photocrosslinked alginate hydrogels for nucleus pulposus cell encapsulation. *J Biomed Mater Res A*. 2009;91(1):187-194.
59. Varma DM, Lin HA, Long RG, et al. Thermoresponsive, redox-polymerized cellulosic hydrogels undergo in situ gelation and restore intervertebral disc biomechanics post discectomy. *Eur Cell Mater*. 2018;35:300-317.
60. Joshi A, Fussell G, Thomas J, et al. Functional compressive mechanics of a PVA/PVP nucleus pulposus replacement. *Biomaterials*. 2006; 27(2):176-184.
61. Lin HA, Gupta MS, Varma DM, Gilchrist ML, Nicoll SB. Lower cross-linking density enhances functional nucleus pulposus-like matrix elaboration by human mesenchymal stem cells in carboxymethylcellulose hydrogels. *J Biomed Mater Res A*. 2016;104(1):165-177.
62. Varma DM, DiNicolas MS, Nicoll SB. Injectable, redox-polymerized carboxymethylcellulose hydrogels promote nucleus pulposus-like extracellular matrix elaboration by human MSCs in a cell density-dependent manner. *J Biomater Appl*. 2018;33(4):576-589.
63. Leone G, Torricelli P, Chiumiento A, Facchini A, Barbucci R. Amidic alginate hydrogel for nucleus pulposus replacement. *J Biomed Mater Res A*. 2008;84(2):391-401.

64. Chaudhuri O, Gu L, Klumpers D, et al. Hydrogels with tunable stress relaxation regulate stem cell fate and activity. *Nat Mater.* 2016; 15(3):326-334.
65. Kettler A, Kaps HP, Haegele B, Wilke HJ. Biomechanical behavior of a new nucleus prosthesis made of knitted titanium filaments. *Sas J.* 2007;1(4):125-130.
66. Khoushabi A, Wyss CS, Caglar B, Pioletti D, Bourban PE. Tailoring swelling to control softening mechanisms during cyclic loading of PEG/cellulose hydrogel composites. *Compos Sci Technol.* 2018;168: 88-95.
67. Lin HA, Varma DM, Hom WW, et al. Injectable cellulose-based hydrogels as nucleus pulposus replacements: Assessment of in vitro structural stability, ex vivo herniation risk, and in vivo biocompatibility. *J Mech Behav Biomed Mater.* 2019;96:204-213.
68. Mansour JM. Biomechanics of cartilage. *Kinesiology: the mechanics and pathomechanics of human movement.* 2003;2:66-79.
69. Gupta MS, Nicoll SB. Functional nucleus pulposus-like matrix assembly by human mesenchymal stromal cells is directed by macromer concentration in photocrosslinked carboxymethylcellulose hydrogels. *Cell Tissue Res.* 2014;358(2):527-539.
70. Smith LJ, Gorth DJ, Showalter BL, et al. In vitro characterization of a stem-cell-seeded triple-interpenetrating-network hydrogel for functional regeneration of the nucleus pulposus. *Tissue Eng Part A.* 2014; 20(13-14):1841-1849.
71. Fernandez C, Marionneaux A, Gill S, Mercuri J. Biomimetic nucleus pulposus scaffold created from bovine caudal intervertebral disc tissue utilizing an optimal decellularization procedure. *J Biomed Mater Res A.* 2016;104(12):3093-3106.
72. Cortes DH, Jacobs NT, DeLucca JF, Elliott DM. Elastic, permeability and swelling properties of human intervertebral disc tissues: A benchmark for tissue engineering. *J Biomech.* 2014;47(9):2088-2094.
73. Rasouljan A, Vakili-Tahami F, Smit TH. Linear and nonlinear biphasic mechanical properties of goat IVDs under different swelling conditions in confined compression. *Ann Biomed Eng.* 2021;49(12): 3296-3309.
74. Strange DG, Oyen ML. Composite hydrogels for nucleus pulposus tissue engineering. *J Mech Behav Biomed Mater.* 2012;11:16-26.
75. Chan AH, Boughton PC, Ruys AJ, Oyen ML. An interpenetrating network composite for a regenerative spinal disc application. *J Mech Behav Biomed Mater.* 2017;65:842-848.
76. Cacopardo L, Guazzelli N, Nossa R, Mattei G, Ahluwalia A. Engineering hydrogel viscoelasticity. *J Mech Behav Biomed Mater.* 2019;89: 162-167.
77. Almdal K, Dyre J, Hvidt S, Kramer O. Towards a phenomenological definition of the term 'gel'. *Poly Gels Netw.* 1993;1(1):5-17.
78. Wan S, Borland S, Richardson SM, Merry CLR, Saiani A, Gough JE. Self-assembling peptide hydrogel for intervertebral disc tissue engineering. *Acta Biomater.* 2016;46:29-40.
79. Su WY, Chen YC, Lin FH. Injectable oxidized hyaluronic acid/adipic acid dihydrazide hydrogel for nucleus pulposus regeneration. *Acta Biomater.* 2010;6(8):3044-3055.
80. Iatridis JC, Weidenbaum M, Setton LA, Mow VC. Is the nucleus pulposus a solid or a fluid? mechanical behaviors of the nucleus pulposus of the human intervertebral disc. *Spine.* 1996;21(10):1174-1184.
81. Leahy JC, Hukins DWL. Viscoelastic properties of the nucleus pulposus of the intervertebral disk in compression. *J Mater Sci Mater Med.* 2001;12(8):689-692.
82. Berlemann U, Schwarzenbach O. An injectable nucleus replacement as an adjunct to microdiscectomy: 2 year follow-up in a pilot clinical study. *Eur Spine J.* 2009;18(11):1706-1712.
83. Tsaryk R, Gloria A, Russo T, et al. Collagen-low molecular weight hyaluronic acid semi-interpenetrating network loaded with gelatin microspheres for cell and growth factor delivery for nucleus pulposus regeneration. *Acta Biomater.* 2015;20:10-21.
84. Ligorio C, Zhou M, Wychowanec JK, et al. Graphene oxide containing self-assembling peptide hybrid hydrogels as a potential 3D injectable cell delivery platform for intervertebral disc repair applications. *Acta Biomater.* 2019;92:92-103.
85. Wang Y, Zhang Y, Chen K, et al. Injectable nanostructured colloidal gels resembling native nucleus pulposus as carriers of mesenchymal stem cells for the repair of degenerated intervertebral discs. *Mater Sci Eng C: Mater Biol Appl.* 2021;128:112343.
86. Jia H, Lin X, Wang D, et al. Injectable hydrogel with nucleus pulposus-matched viscoelastic property prevents intervertebral disc degeneration. *J Orthopaed Transl.* 2022;33:162-173.
87. Gloria A, Borzacchiello A, Causa F, Ambrosio L. Rheological characterization of hyaluronic acid derivatives as injectable materials toward nucleus pulposus regeneration. *J Biomater Appl.* 2012;26(6):745-759.
88. Feilden E, Blanca EGT, Giuliani F, Saiz E, Vandepierre L. Robocasting of structural ceramic parts with hydrogel inks. *J Eur Ceram Soc.* 2016;36(10):2525-2533.
89. Thakur A, Jaiswal MK, Peak CW, et al. Injectable shear-thinning nanoengineered hydrogels for stem cell delivery. *Nanoscale.* 2016; 8(24):12362-12372.
90. Ligorio C, Vijayaraghavan A, Hoyland JA, Saiani A. Acidic and basic self-assembling peptide and peptide-graphene oxide hydrogels: characterisation and effect on encapsulated nucleus pulposus cells. *Acta Biomater.* 2022;143:145-158.
91. Joshi A, Vresilovic E, Marcolongo M, Lowman A, Karduna A. The effect of hydrogel nucleus implant on the mechanical behavior of the lumbar functional spinal unit: An experimental study. *Proceedings of the IEEE Annual Northeast Bioengineering Conference (NEBEC).* 2003.
92. Shaha RK, Merkel DR, Anderson MP, et al. Biocompatible liquid-crystal elastomers mimic the intervertebral disc. *J Mech Behav Biomed Mater.* 2020;107:103757.
93. Li Z, Kaplan KM, Wertzel A, et al. Biomimetic fibrin-hyaluronan hydrogels for nucleus pulposus regeneration. *Regen Med.* 2014;9(3):309-326.
94. Pérez-San Vicente A, Peroglio M, Ernst M, et al. Self-healing dynamic hydrogel as injectable shock-absorbing artificial nucleus pulposus. *Biomacromolecules.* 2017;18(8):2360-2370.
95. Guo W, Douma L, Hu MH, et al. Hyaluronic acid-based interpenetrating network hydrogel as a cell carrier for nucleus pulposus repair. *Carbohydr Polym.* 2022;277:118828.
96. Christiani T, Mys K, Dyer K, Kadlowec J, Iftode C, Vernengo AJ. Using embedded alginate microparticles to tune the properties of in situ forming poly(N-isopropylacrylamide)-graft-chondroitin sulfate bioadhesive hydrogels for replacement and repair of the nucleus pulposus of the intervertebral disc. *JOR Spine.* 2021;4(3): e1161.
97. Shi Y, Wang K, Feng X, et al. Additive manufactured self-powered mechanolectric sensor as the artificial nucleus pulposus for monitoring tissue rehabilitation after discectomy. *Nano Energy.* 2022;96:107113.
98. Khandaker M, Riahanizad S. Evaluation of Electrospun Nanofiber-Anchored Silicone for the Degenerative Intervertebral Disc. *J Healthc Eng.* 2017;2017:5283846.
99. Kamatani T, Hagizawa H, Yarimitsu S, et al. Human iPSC cell-derived cartilaginous tissue spatially and functionally replaces nucleus pulposus. *Biomaterials.* 2022;284:121491.
100. Wilke HJ, Wenger K, Claes L. Testing criteria for spinal implants: recommendations for the standardization of in vitro stability testing of spinal implants. *Eur Spine J.* 1998;7(2):148-154.
101. Schmitz TC, Salzer E, Crispim JF, et al. Characterization of biomaterials intended for use in the nucleus pulposus of degenerated intervertebral discs. *Acta Biomater.* 2020;114:1-15.
102. Moss IL, Gordon L, Woodhouse KA, Whyne CM, Yee AJM. A novel thiol-modified hyaluronan and elastin-like polypeptide composite material for tissue engineering of the nucleus pulposus of the intervertebral disc. *Spine (Phila, Pa 1976).* 2011;36(13):1022-1029.

103. Foss BL, Maxwell TW, Deng Y. Chondroprotective supplementation promotes the mechanical properties of injectable scaffold for human nucleus pulposus tissue engineering. *J Mech Behav Biomed Mater*. 2014;29:56-67.
104. Piening LM, Lillyman DJ, Lee FS, Lozano AM, Miles JR, Wachs RA. Injectable decellularized nucleus pulposus tissue exhibits neuroinhibitory properties. *JOR Spine*. 2022;5(1):e1187.
105. Silva-Correia J, Gloria A, Oliveira MB, et al. Rheological and mechanical properties of acellular and cell-laden methacrylated gellan gum hydrogels. *J Biomed Mater Res A*. 2013;101(12):3438-3446.
106. Leone G, Consumi M, Lamponi S, et al. Hybrid PVA-xanthan gum hydrogels as nucleus pulposus substitutes. *Int J Polym Mater Polym Biomater*. 2019;68(12):681-690.
107. Gan Y, Li P, Wang L, et al. An interpenetrating network-strengthened and toughened hydrogel that supports cell-based nucleus pulposus regeneration. *Biomaterials*. 2017;136:12-28.
108. Francisco AT, Mancino RJ, Bowles RD, et al. Injectable laminin-functionalized hydrogel for nucleus pulposus regeneration. *Biomaterials*. 2013;34(30):7381-7388.
109. Xu P, Guan J, Chen Y, et al. Stiffness of photocrosslinkable gelatin hydrogel influences nucleus pulposus cell properties in vitro. *J Cell Mol Med*. 2021;25(2):880-891.
110. Frith JE, Menzies DJ, Cameron AR, et al. Effects of bound versus soluble pentosan polysulphate in PEG/HA-based hydrogels tailored for intervertebral disc regeneration. *Biomaterials*. 2014;35(4):1150-1162.
111. Yu L, Liu Y, Wu J, et al. Genipin cross-linked decellularized nucleus pulposus hydrogel-like cell delivery system induces differentiation of ADSCs and retards intervertebral disc degeneration. *Front Bioeng Biotechnol*. 2021;9:9.
112. Gullbrand SE, Schaer TP, Agarwal P, et al. Translation of an injectable triple-interpenetrating-network hydrogel for intervertebral disc regeneration in a goat model. *Acta Biomater*. 2017;60:201-209.
113. Lee T, Lim TH, Lee SH, Kim JH, Hong J. Biomechanical function of a balloon nucleus pulposus replacement system: A human cadaveric spine study. *J Orthop Res*. 2018;36(1):167-173.
114. Chen X, Tan B, Wang S, et al. Rationally designed protein cross-linked hydrogel for bone regeneration via synergistic release of magnesium and zinc ions. *Biomaterials*. 2021;274:120895.
115. Pereira DR, Silva-Correia J, Caridade SG, et al. Development of gellan gum-based microparticles/hydrogel matrices for application in the intervertebral disc regeneration. *Tissue Eng Part C Methods*. 2011;17(10):961-972.
116. Jones JR. Review of bioactive glass: From Hench to hybrids. *Acta Biomater*. 2013;9(1):4457-4486.
117. Halloran DO, Grad S, Stoddart M, Dockery P, Alini M, Pandit AS. An injectable cross-linked scaffold for nucleus pulposus regeneration. *Biomaterials*. 2008;29(4):438-447.
118. Vernengo J, Fussell GW, Smith NG, Lowman AM. Evaluation of novel injectable hydrogels for nucleus pulposus replacement. *J Biomed Mater Res B Appl Biomater*. 2008;84(1):64-69.
119. Thomas JD, Fussell G, Sarkar S, Lowman AM, Marcolongo M. Synthesis and recovery characteristics of branched and grafted PNIPAAm-PEG hydrogels for the development of an injectable load-bearing nucleus pulposus replacement. *Acta Biomater*. 2010;6(4):1319-1328.
120. Bader RA, Rochefort WE. Rheological characterization of photopolymerized poly(vinyl alcohol) hydrogels for potential use in nucleus pulposus replacement. *J Biomed Mater Res A*. 2008;86(2):494-501.
121. Reza AT, Nicoll SB. Characterization of novel photocrosslinked carboxymethylcellulose hydrogels for encapsulation of nucleus pulposus cells. *Acta Biomater*. 2010;6(1):179-186.
122. Schmocker A, Khoushabi A, Farahi S, et al. Multi-scale modeling of photopolymerization for medical hydrogel-implant design. In *Progress in Biomedical Optics and Imaging – Proceedings of SPIE*. 2013.
123. Schmocker A, Khoushabi A, Pioletti DP, Bourban PE, Manson JA, Moser C. Mechanical properties of a photopolymerizable hydrogel for intervertebral disc replacement. in *ASME International Mechanical Engineering Congress and Exposition. Proceedings (IMECE)*. 2013.
124. Francisco AT, Hwang PY, Jeong CG, Jing L, Chen J, Setton LA. Photocrosslinkable laminin-functionalized polyethylene glycol hydrogel for intervertebral disc regeneration. *Acta Biomater*. 2014;10(3):1102-1111.
125. Binetti VR, Fussell GW, Lowman AM. Evaluation of two chemical crosslinking methods of poly(vinyl alcohol) hydrogels for injectable nucleus pulposus replacement. *J Appl Polym Sci*. 2014;131(19):40843.
126. Zhang H, Xia H, Zhao Y. Poly(vinyl alcohol) hydrogel can autonomously self-heal. *ACS Macro Lett*. 2012;1(11):1233-1236.
127. Talebian S, Mehrali M, Taebnia N, et al. Self-Healing Hydrogels: The Next Paradigm Shift in Tissue Engineering? *Adv Sci*. 2019;6(16):1801664.
128. Tallia F, Russo L, Li S, et al. Bouncing and 3D printable hybrids with self-healing properties. *Mater Horiz*. 2018;5(5):849-860.
129. Husson JL, Korge A, Polard JL, Nydegger T, Kneubühler S, Mayer HM. A memory coiling spiral as nucleus pulposus prosthesis – concept, specifications, bench testing, and first clinical results. *J Spinal Disord Tech*. 2003;16(4):405-411.
130. Tendulkar G, Sreekumar V, Rupp F, et al. Characterisation of porous knitted titanium for replacement of intervertebral disc nucleus pulposus. *Sci Rep*. 2017;7(1):16611.
131. Zengerle L, Köhler A, Debout E, Hackenbroch C, Wilke HJ. Nucleus replacement could get a new chance with annulus closure. *Eur Spine J*. 2020;29(7):1733-1741.
132. Trappmann B, Baker BM, Polacheck WJ, Choi CK, Burdick JA, Chen CS. Matrix degradability controls multicellularity of 3D cell migration. *Nat Commun*. 2017;8(1):371.
133. Thomé C, Kuršumović A, Klassen PD, et al. Effectiveness of an Annular Closure Device to Prevent Recurrent Lumbar Disc Herniation: A Secondary Analysis With 5 Years of Follow-up. *JAMA Netw Open*. 2021;4(12):e2136809.
134. Sharifi S, van Kooten TG, Kranenburg HJC, et al. An annulus fibrosus closure device based on a biodegradable shape-memory polymer network. *Biomaterials*. 2013;34(33):8105-8113.
135. Bateman AH, Balkovec C, Akens MK, et al. Closure of the annulus fibrosus of the intervertebral disc using a novel suture application device-in vivo porcine and ex vivo biomechanical evaluation. *Spine J*. 2016;16(7):889-895.

SUPPORTING INFORMATION

Additional supporting information can be found online in the Supporting Information section at the end of this article.

How to cite this article: Li ZL, Lu Q, Honiball JR, Wan SH-T, Yeung KW-K, Cheung KM-C. Mechanical characterization and design of biomaterials for nucleus pulposus replacement and regeneration. *J Biomed Mater Res*. 2023;111(12):1888-1902. doi:10.1002/jbm.a.37593